

# Supporting Information

Niu et al. 10.1073/pnas.1007276107

## SI Materials and Methods

**Strains and Growth Conditions.** Bacterial strains and plasmids used in this study are listed in Table S1. All cloning was performed using *Escherichia coli* strain JM109. For purifying proteases, *Bacillus nematocida* strain B16 was cultured in YPD medium (1% yeast extract/2% peptone/2% dextrose) (1, 2). For preparing all other strains and treatments, bacteria were grown in LB medium at 37 °C, and, when appropriate, kanamycin (50 µg/mL), chloramphenicol (5 µg/mL), tetracycline (50 µg/mL), or ampicillin (100 µg/mL) was added to the medium.

*Caenorhabditis elegans* nematodes were grown for 4–7 d at room temperature (11–28 °C) on oatmeal agar medium. The cultured nematodes were separated using the Baerman funnel technique (3), and an aqueous suspension of the nematode was prepared as a working stock.

**DNA Manipulations.** The gene-specific primers used in this study are listed in Table S2. Construction of gene-disruption strains followed a previously reported protocol (4). Plasmid vectors pSG1170 (5) and pSG1194 (6) were used for the construction of strains expressing *gfp*- and *dsRed*-tagged proteases, respectively. These plasmids were kindly provided by Daniel R. Zeigler (The Ohio State University, Columbus, OH) and allowed fusion of *gfp* and *dsRed* to the 3' end of the genes of interest. The recombinant plasmids were transformed into competent cells of *B. nematocida* following the protocols supplied by the *Bacillus* Genetic Stock Center, Department of Biochemistry, Ohio State University, Columbus, OH.

To construct the *E. coli* strain expressing GFP as the negative control, the gene encoding EGFP was amplified through PCR from the plasmid pEGFP-C1 using the primers *egfp*for and *egfp*rev. The amplified 716-bp fragment was purified from agarose gel and then was ligated into *E. coli* pMD19-T vector to generate the T-EGFP plasmid. The plasmid was transformed into *E. coli* strain JM109 competent cells.

**Western Blot Analysis.** Western blot hybridization followed techniques described in ref. 7. Polyclonal antibodies against Bace16 and Bae16 were prepared by the Laboratory for Monoclonal Antibodies in Yunnan University, Yunnan, People's Republic of China, and were used at a 1:500 dilution. GFP antibody (Cell Signaling Technology) and a purified mouse anti-DsRed monoclonal antibody (BD Pharmingen) were used at a 1:1,000 dilution. Goat anti-mouse secondary antibody conjugated with HRP (Bio-Rad) or a peroxidase-conjugated goat anti-rabbit IgG (H+L) (1:5000) (Bio-Rad) was used in the detection assay. Position of the bound antibodies was detected using chemiluminescence (ECL; Amersham Biosciences/GE Healthcare) substrates.

**Proteolytic Activity Assay.** Protease activities of the culture filtrate first were analyzed qualitatively using the casein plate method described by Zhao et al. (8). Quantitative analysis of protease activity was determined using the caseinolytic method described by Niu et al. (1). Protein concentration was determined following that of Bradford (9), and BSA was used as the standard.

**Infection of Nematodes.** The method for determining nematocidal activity (NA) was based on those described previously (1, 9, 10). Briefly, nematodes were washed thoroughly with a 10 mM sterile PBS (pH 7.0), and a suspension containing 40–50 nematodes (20 µL) was transferred to a sterile 1.5-mL Eppendorf tube. Samples including filtrates of bacterial strains and purified proteases were added individually to the nematodes for infectivity testing. After the

mixture was incubated at room temperature (11–28 °C) for intervals ranging from 4 to 60 h, dead nematodes were counted, and nematode mortality was calculated. At least five nematodes were sampled randomly from the Eppendorf tube at different time intervals during the protease localization assay. The sampled nematodes then were pretreated with 10 mM PBS buffer (pH 7.0) for 30 min at room temperature followed by three washes (10 min each) in sterile water before examination under fluorescent microscopy.

Bacterial infection of nematodes also was performed using a modified dialysis membrane technique (11). Briefly, pieces of autoclaved cellophane paper were placed on top of agar plates (2%) containing low-nutrient mineral salt to simulate the natural environment and to prevent nematodes from moving into the medium. Bacteria were inoculated onto the cellophane paper and incubated at 28 °C for 7–10 d. The nematodes then were placed in the middle of the plate. Each plate was divided into 20 panes, and the nematodes were selected randomly from 5 of the 20 panes at different time intervals. Nematodes were washed and then tested for infection by the various bacterial strains. The nonpathogenic bacteria *E. coli* strain GF109 and uninoculated medium were used as negative controls.

All infection experiments were performed in triplicate and were repeated at least three times.

**Surface Sterilizing.** Colonization of bacteria was assessed by surface sterilizing according to the literature (12). Nematodes then were washed three to five times using sterile PBS (pH 7.5) until colonization was not detected (i.e., when no growth was observed from rinse solution inoculated onto plates with antibiotics).

**Ultra-Structural Analyses of Bacterial Infection Against Nematodes Using SEM and Transmission Electron Microscopic Examinations.** For environmental SEM examinations, nematodes from bioassay experiments were washed three times in phosphate buffer (pH 7.0) and were fixed in 4% glutaraldehyde for 2 h and then in 2% osmic acid for 40–60 min. After dehydration in a series of ethanol solutions, the samples were dried, sputter-coated with gold, and examined under SEM (Philips XL30) in the environmental mode operating at 10–20 kV.

For transmission electron microscopic (TEM) examinations, nematodes from various treatments were fixed overnight in a solution of 2% glutaraldehyde plus 4% paraformaldehyde in 0.1 M Sorensen phosphate buffer (pH 7.4). The specimens were post-fixed in the dark for 2 h in 1% osmium tetroxide, stained *en bloc* with an aqueous solution of 5% uranyl acetate for 2 h, dehydrated in acetone, embedded in araldite, and sectioned and stained with a saturated solution of uranyl acetate in 50% ethanol and then with lead citrate in 0.2% NaOH. Electron micrographs were obtained under a Philips CM 100 TEM.

**Microinjection Procedure.** The crude protease was extracted according to the methods described previously (1). For nematode microinjection, an electric IM-30 microinjector (Narishige), linked to a stereoscopic microscope Nikon eclipse TS100, was used with an air entrance pressure of 3.5 bars. Needles for microinjection were made in a puller (Narishige PB-7) using glass capillaries with an internal filament (1 mm external diameter, 0.6 mm internal diameter) (GD-1; Narishige) and an EG-400 microgrinder (Narishige). Pasteur pipettes were shaped by heat until they fit inside the needles for loading protease solutions.

During injection, nematodes were held onto agar disks (20 mL of 1.5% agarose) placed in 35-mm Petri dishes. The disks contained 1-mm parallel grooves which were generated by hot glass

capillaries (13). Adult *C. elegans* were anesthetized in a stream of ether. The anesthetized worms were arranged carefully in line in halocarbon oil 700 (50 mL; Sigma H8898) and were pressed gently into the grooves before microinjection through the mouth. Nematodes microinjected with the same quantities of PBS (20 mM, pH 7.0) and GFP served as negative controls.

At various time points after microinjection, nematodes were mounted on glass slides with sterile water and examined under a Nikon E800 microscope equipped for epifluorescence with a mercury lamp. GFP fluorescence was visualized with an excitation filter of 450–490 nm (blue light) and a barrier filter of 515 nm. The absorption spectrum of DsRed displays a strong peak located at 559 nm and two additional shoulders at 524 nm and 485 nm. Independent of the excitation wavelength, a major fluorescence at 583 nm also was observed in our samples. Micrographs were recorded with an Olympus camera coupled to an exposure control unit, using the NIS-Elements BR 2.30 software (Nikon).

**Assays of Nematode-Attracting Ability and NA in Soil.** To determine the nematode-attracting ability (AA) of the tested bacteria in soil, soil samples were collected near a park close to the Yunnan University campus. The protocol for the AA assay in soil was as follows (Fig. 4A). Soil samples were placed in Petri dishes, and aliquots of bacteria were inoculated at the center of the dish. Adult *C. elegans* then were placed 3 cm away from the center. At different time intervals, soil samples were taken about 1 cm away from the center, and the number of nematodes in the sample was counted under a microscope.

The NA in soil was determined following a protocol of Luo et al. (14) with the following modifications. First, samples were taken at multiple spots around sites A, B, and C, corresponding to distances of 3 cm, 2 cm, and 1 cm, respectively, between nematodes and site of bacteria inoculation. Second, strain B19 was cultured in LB medium until OD<sub>650</sub> reached 0.4–0.6. Third, 5-g aliquots of soil were inoculated with three different volumes of bacteria inoculum (inoculum 1, 5 µL; inoculum 2, 10 µL, or inoculum 3, 15 µL of the original culture). The bacteria-inoculated soil samples were mixed gently with ≈500 *Panagrellus redivivus* nematodes in 200 µL of water in a Petri dish. The soil-bacteria-nematode mixtures were kept at room temperature and a constant humidity for 4 d. The worms then were washed from the soil, and the number of dead and live adult nematodes was counted under a microscope. Soil samples without bacterial inoculation were used as negative controls. This experiment was conducted twice with three replicates each.

## SI Results

Fig. S1 shows the results of the attractant experiment using inverted Petri dishes. Fig. S2 shows the results of the gas chromatography (GC)/MS total ion current traces from different samples. Fig. S3 shows that gut tissue in *C. elegans* was damaged after swallowing *B. nematocida* but not after swallowing *E. coli*. Fig. S7 shows 2D electrophoresis maps of intestinal proteins of *C. elegans*.

**Confirmation of Gene-Knockout Mutants by PCR and Western Blot Analysis.** PCR analysis showed that two amplicons of approximately 4.9 kb (gene *vΔbae16*) and 4.5 kb (gene *vΔbace16*) were both found in the double-knockout strain B13-1 (Fig. S4A, lanes 1 and 2). Furthermore, Western blot analysis revealed that neither the Bace16 polyclonal antibody nor the Bae16 polyclonal antibody could detect the corresponding proteins on the PVDF membrane (Fig. S4B, lanes 1 and 4), confirming the successful knockout of both genes in strain B13. Similarly, in the *bae16*-knockout strain B14, only gene *vΔbae16* was amplified (Fig. S4A, lane 3), and Western blot analysis displayed a 28-kDa protein band of the culture supernatant from strain B14 when reacted with the Bace16 polyclonal antibody (Fig. S4B, lane 2), but no signal was detected when Bae16 polyclonal antibody was used (Fig. S4B, lane 5). Similarly, in the *bace16*-knockout strain B15, only gene *vΔbace16* was amplified (Fig. S4A, lane 4). Western blot analysis displayed a 40-kDa protein band when reacted with Bae16 polyclonal antibody (Fig. S4B, lane 3), and no signal was observed when Bace16 polyclonal antibody was used (Fig. S4B, lane 6).

**PCR and Western Blot Analyses Confirmed Successful Construction of the Transformants Expressing Fluorescent-Tagged Proteases.** PCR analysis showed that amplicons of about 1.8 kb (*vbace17*) and/or 1.9 kb (*vbae18*) were found in the transformants B19, B18, and B17 (Fig. S5A, lanes 3–6), whereas the negative controls of wild-type strain B16 had no amplified product (Fig. S5A, lanes 1–2). The presence of Bace16-GFP and Bae16-DsRed fusion proteins of the expected sizes was confirmed further by Western blot analysis (Fig. S5B and C). For the double-fluorescent strain B19, using either the specific anti-GFP (or anti-DsRed) antibody or the antiserum produced by Bace16 (or Bae16), we detected a cross-reacting band of similar intensity at approximate molecular weight (MW) 55 kDa (or 71 kDa) (Fig. S5B, lanes 4 and 8, and Fig. S5C, lanes 4 and 8). These results indicated that strain B19 expressing C-terminal GFP fusion to Bace16 and C-terminal DsRed fusion to Bae16 was constructed successfully. Meanwhile, the negative control *E. coli* GF109 strain displayed a 27-kDa GFP protein band in the Western blot analysis (Fig. S5B, lane 9).

**Intestinal Localization of the Proteases.** In the localization experiments, we put the tested nematodes onto the lawn of different bacterial strains for 24 h. The *E. coli* strain GF109 exhibited the characteristic green fluorescence, but no fluorescence was detected on the tested nematode *C. elegans* after washing with PBS buffer (Fig. S6A). After washing, *C. elegans* treated with the transformants B17, B18, and B19 displayed strong fluorescence on the cuticles and within the intestines (Fig. S6B–D). More RFP (Bace16) was detected within the intestine than on the cuticle (Fig. S6B and D), whereas GFP (Bae16) showed strong fluorescence in both the intestine and the cuticle (Fig. S6C and D).

- Niu QH, et al. (2006) *Bacillus* sp. B16 kills nematodes with a serine protease identified as a pathogenic factor. *Appl Microbiol Biotechnol* 69:722–730.
- Niu QH, et al. (2006) A neutral protease from *Bacillus nematocida*, another potential virulence factor in the infection against nematodes. *Arch Microbiol* 185:439–448.
- Gray NF (1984) Ecology of nematophagous fungi: Comparison of the soil sprinkling method with the Baerman funnel technique in the isolation of endoparasites. *Soil Biol Biochem* 16:81–83.
- Niu QH, et al. (2007) Functional identification of the gene *bace16* from nematophagous bacterium *Bacillus nematocida*. *Appl Microbiol Biotechnol* 75:141–148.
- Lewis PJ, Marston AL (1999) GFP vectors for controlled expression and dual labelling of protein fusions in *Bacillus subtilis*. *Gene* 227:101–110.
- Lewis PJ, Errington J (1996) Use of green fluorescent protein for detection of cell-specific gene expression and subcellular protein localization during sporulation in *Bacillus subtilis*. *Microbiology* 142:733–740.
- Molecular Cloning: A Laboratory Manual* (1989) 2nd Ed (Cold Spring Harbor Laboratory, Cold Spring Harbor, NY).
- Zhao ML, Mo MH, Zhang KQ (2004) Characterization of a neutral serine protease and its full-length cDNA from the nematode-trapping fungus *Arthrobotrys oligospora*. *Mycologia* 96:16–22.
- Bradford MM (1976) A rapid and sensitive method for the quantitation of microgram quantities of protein utilizing the principle of protein-dye binding. *Anal Biochem* 72:248–254.
- Lopez-Llorca LV, Robertson W (1992) Immunocytochemical localization of a 32 kDa protease from the nematophagous fungus *Verticillium suchlasporium* in infected nematode eggs. *Exp Mycol* 16:261–267.
- Ahman J, et al. (2002) Improving the pathogenicity of a nematode-trapping fungus by genetic engineering of a subtilisin with nematotoxic activity. *Appl Environ Microbiol* 68:3408–3415.
- Ciche TA, Darby C, Ehlers R-U, Forst S, Goodrich-Blair H (2006) Dangerous liaisons: The symbiosis of entomopathogenic nematodes and bacteria. *Biol Control* 38:22–46.
- Westerfield M (1993) *The Zebrafish Book: A Guide for the Laboratory Use of Zebrafish (Brachydanio rerio)* (Univ of Oregon Press, Eugene, OR).
- Luo H, Li X, Li G, Pan Y, Zhang K (2006) Acanthocytes of *Stropharia rugosoannulata* function as a nematode-attacking device. *Appl Environ Microbiol* 72:2982–2987.

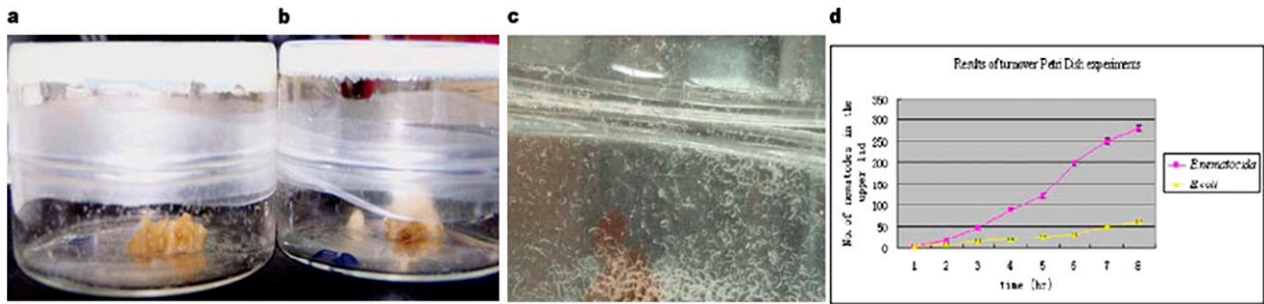


**Fig. S1.** The inverted Petri dish attractant experiment. *B. nematocida* strain B16 (A) or *E. coli* (B) lawns were grown on agar layers in Petri dish lids that then were inverted over lids of the same size containing *C. elegans*. (A) One hundred thirty worms climbed the Petri dish walls toward the strain B16 lawn. (B) Forty-eight worms climbed toward the *E. coli* lawn. (C) Close-up of the climbing worms attracted by strain B16. (D) Graphic representation of the number of nematodes that climbed toward the upper dishes within 8 h.

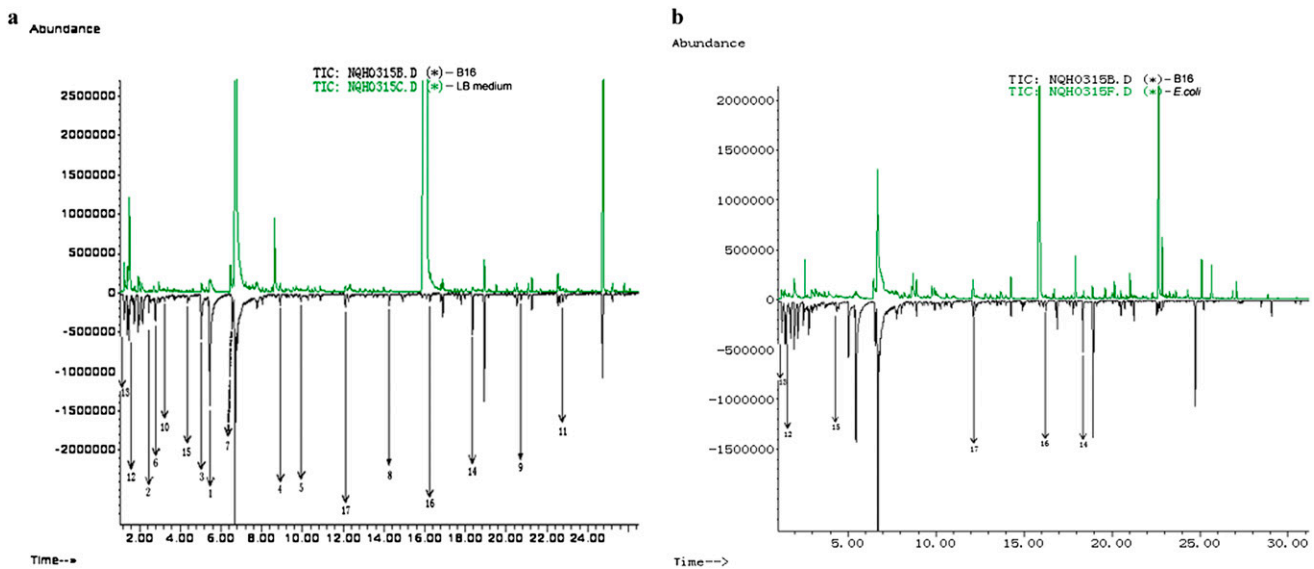


**Fig. S2.** Attractants were determined with GC-MS by comparing the total ion current traces from the pathogenic bacterium *B. nematocida* strain B16, food bacterium *E. coli*, and blank medium. (A) A reverse-overlay map of GC-MS total ion current traces of *B. nematocida* B16 (black) and LB medium (green). The 17 arrows indicate the candidate attractants produced by *B. nematocida* B16. (B) A reverse-overlay map of *B. nematocida* B16 (black) and *E. coli* (green). The six arrows indicate the candidate attractants shared by *B. nematocida* B16 and *E. coli*.

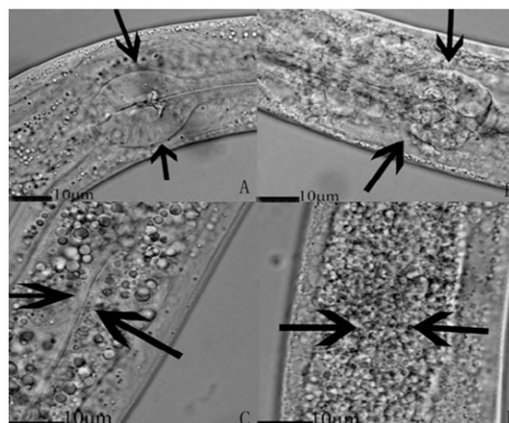


**Fig. S3.** Damaged gut tissue in *C. elegans* after swallowing *B. nematocida* (B and D). In contrast, no damage in gut tissue was observed in *C. elegans* after swallowing *E. coli* (A and C). Micrographs were taken 3 h after worms arrived on the respective bacterial lawns. Arrows point to damaged regions in B and D and the corresponding healthy regions in A and C.



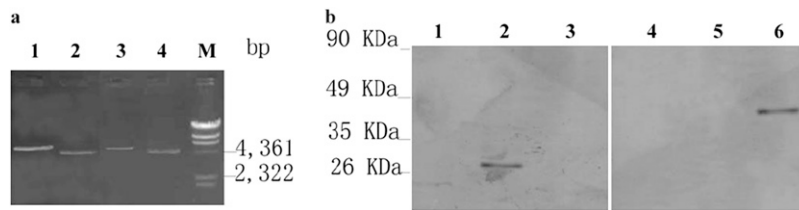


**Fig. 54.** PCR and Western blot analysis of transformants of *bae16* and *bace16* gene-knockout mutants. (A) The PCR products of the three gene-knockout mutants B13, B14, and B15 were analyzed by 0.8% agarose gel electrophoresis using the primers located in the integration vector and target genes, respectively. Lanes 1 and 2,  $\Delta bae16$  and  $\Delta bace16$  in *B. nematocida* strain B13; lane 3,  $\Delta bae16$  in *B. nematocida* strain B14; lane 4,  $\Delta bae16$  in *B. nematocida* strain B15. M, molecular marker. (B) Detection of protease Bace16 using anti-Bace16 polyclonal antibody (lanes 1–3) and detection of protease Bae16 using anti-Bae16 polyclonal antibody (lanes 4–6) in gene-knockout mutants B13, B14, and B15: Lanes 1 and 4 show that neither Bace16 nor Bae16 was detected in the double-mutant B13; lanes 2 and 5 show that only Bace16 (MW 28 kDa) was detected in the *bae16*-deficient mutant B14; lanes 3 and 6 show that only Bae16 (MW 40 kDa) was detected in the *bace16*-deficient mutant B15.

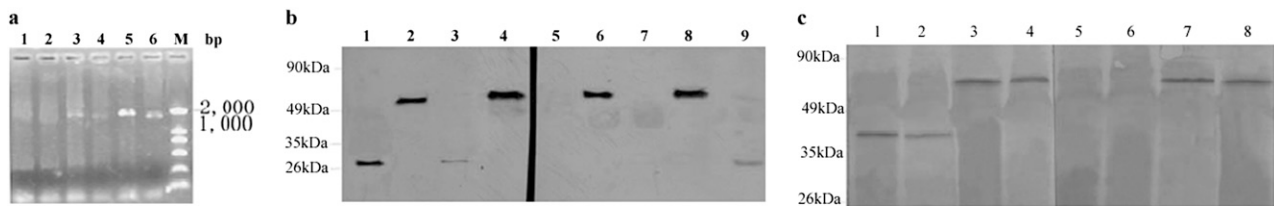


**Fig. 55.** Detection of fusion protein in *B. nematocida* transformants by PCR and Western blot analysis. (A) Analysis of PCR products of the transformants B19, B18, and B17 using 1.0% agarose gel electrophoresis. Lanes 1 and 2 show that the wild-type strain B16 has no amplicon for *vbae16* and *vbace16*; lanes 3 and 4 show that both *vbae16* and *vbace16* are amplified in the double-fusion strain B19; lane 5, *vbae16* in strain B18; lane 6, *vbace16* in strain B17. M, molecular marker. (B) Detection of Bace16 and GFP-fused Bace16 using anti-Bace16 polyclonal antibody and anti-GFP antibody, respectively. Lanes 1–4, respectively, show 28-kDa Bace16 in wild-type strain B16, 55-kDa Bace16-GFP in strain B17, 28-kDa Bace16 in strain B18, and 55-kDa Bace16-GFP in strain B19, hybridized with the anti-Bace16 polyclonal antibody. Lanes 5–9, respectively, show there is no GFP hybridization signal in wild-type strain B16, there is a Bace16-GFP signal in strain B17, there is no hybridization signal in strain B18, there is a Bace16-GFP signal in strain B19, and there is a 27-kDa GFP signal in *E. coli* GF109 with anti-GFP antibody. (C) Detection of Bae16 and DsRed-fused Bae16 using anti-Bae16 polyclonal antibody and anti-DsRed antibody, respectively. Lanes 1–4, respectively, show 40-kDa Bae16 in the wild-type strain, 40-kDa Bae16 in strain B17, 71-kDa Bae16-DsRed in strain B18, and 71-kDa Bae16-DsRed in strain B19 hybridized with anti-Bae16 antibody. Lanes 5–8 show no hybridization signal in wild-type strain B16, no hybridization signal in strain B17, a 71-kDa Bae16-DsRed signal in strain B18, and a 71-kDa Bae16-DsRed signal in strain B19 when hybridized with anti-DsRed antibody.

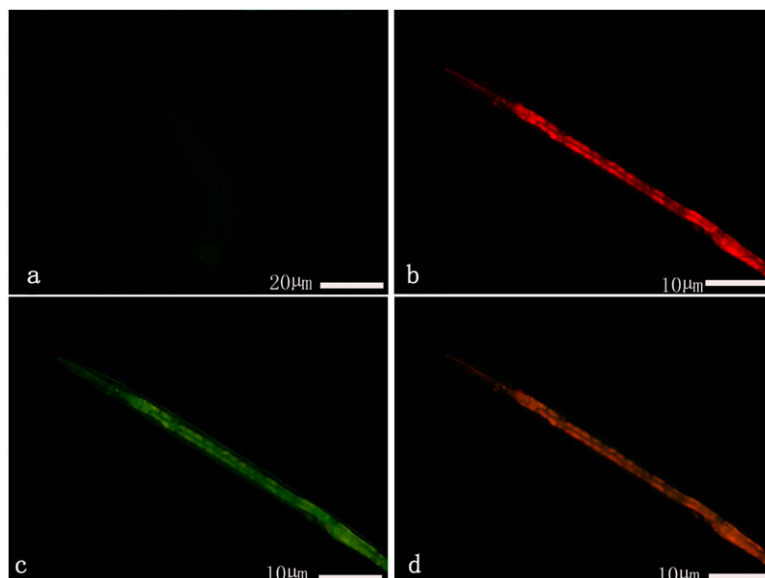


**Fig. 56.** Localization of two proteases during infection. (A) *C. elegans* shows little fluorescence when treated with *E. coli* strain GF109 for 24 h. (B) Intestine of *C. elegans* showed strong Bae16-DsRed fluorescence when treated with *B. nematocida* strain B18 for 24 h. (C) Cuticle and intestine of *C. elegans* showed strong Bace16-GFP fluorescence when treated with *B. nematocida* strain B17 for 24 h. (D) An overlay image treated with the double-localization strain B19.



**Table S1. Strains and plasmids**

Strain or plasmid	Description	Source/construction
<b>Strain</b>		
<i>B. nematocida</i> B13	Double-knockout strain	B16 transformed with pΔbae16 and pΔbace16
<i>B. nematocida</i> B14	Bae16-knockout strain	B16 transformed with pΔbae16
<i>B. nematocida</i> B15	Bace16-knockout strain	B16 transformed with pΔbace16 (1)
<i>B. nematocida</i> B16	Wild type	Laboratory strain
<i>B. nematocida</i> B17	Bace16-localization strain	B16 transformed with pSB17
<i>B. nematocida</i> B18	Bae16-localization strain	B16 transformed with pSB18
<i>B. nematocida</i> B19	Dual-localization strain	B16 transformed with pSB17 and pSB18
<i>E. coli</i> JM109	Competent cell	TaKaRa
<i>E. coli</i> GF109	Localization study for negative control	JM109 transformed with T-EGFP
<b>Plasmid</b>		
pMD19-T	Cloning vector in <i>E. coli</i>	TaKaRa
TB14	Plasmid containing 345bp sequence of <i>bae16</i>	PCR product inserted into pMD19-T
TB15	Plasmid containing 295bp sequence of <i>bace16</i>	PCR product inserted into pMD19-T
pCP115	Gene disruption vector	<i>Bacillus</i> Genetic Stock Center, Department of Biochemistry, Ohio State University, Columbus, OH
pΔbae16	Gene disruption plasmid for <i>bae16</i>	<i>Cla</i> I- <i>Pst</i> I digest of TB14 inserted into large fragment of similarly cut pCP115
pΔbace16	Gene disruption plasmid for <i>bace16</i>	<i>Cla</i> I- <i>Pst</i> I digest of TB15 inserted into large fragment of similarly cut pCP115
pEGFP-C1	Template for amplifying <i>egfp</i>	Clontech
T-EGFP	Expression vector in <i>E. coli</i>	<i>egfp</i> inserted into pMD19-T
pSG1170	Integration vector in B16 Genotype: bla cat lacI Pspac-gfpUV	<i>Bacillus</i> Genetic Stock Center
T-Bace17	Plasmid containing C-terminal 544bp sequence of <i>bace16</i>	PCR product inserted into pMD19-T
pSG1194	Integration vector in B16 Genotype: bla cat lacZ	<i>Bacillus</i> Genetic Stock Center
T-Bae18	Plasmid containing C-terminal 202bp sequence of <i>bae16</i>	PCR product inserted into pMD19-T
pSB17	Gene localization plasmid for <i>bace16</i>	<i>Xho</i> I- <i>EcoR</i> I digest of T-Bace17 inserted into large fragment of similarly cut pSG1170
pSB18	Gene localization plasmid for <i>bae16</i>	<i>EcoR</i> I- <i>Bam</i> HI digest of T-Bae18 inserted into large fragment of similarly cut pSG1194

1. Niu QH, et al. (2007) Functional identification of the gene *bace16* from nematophagous bacterium *Bacillus nematocida*. *Appl Microbiol Biotechnol* 75:141–148.

**Table S2. Gene-specific primers used in this study**

Target gene	Primer	Sequence (5'-3')	Description
<i>bae16A</i> (0.345 kbp)	<i>bae16A</i> for	<u>ATCGATAGCGGCAAATATGTAATGCGTG</u> ( <i>Cla</i> I-link)	To construct plasmid TB14
	<i>bae16A</i> rev	<u>CTGCAGTGAACCGGAAAGAGGCGAGAAG</u> ( <i>Pst</i> I-link)	
<i>vΔbace16</i> (4.5 kbp)	<i>vΔbace16</i> for	GTGAGAGGCAAAAAGGTATGGATC	To verify <i>bace16</i> -mutant
	<i>vΔbace16</i> rev	CTGAGCTGCCGCTGTACGTTGA	
<i>vΔbae16</i> (4.9 kbp)	<i>vΔbae16</i> for	GTGGGTTTAGGTAAGAAATTGTCT	To verify <i>bae16</i> -mutant
	<i>vΔbae16</i> rev	CAATCCAACCTGCATTCCAGGC CG	
<i>bace16F</i> (0.544 kbp)	<i>bace16F</i> for	<u>CTCGAGAGTTCTCGGCGTGACGTTCC</u> ( <i>Xho</i> I-link)	To construct plasmid T-Bace17
	<i>bace16F</i> rev	<u>GAATTCCTGAGCTGCCGCTGTACGTTGA</u> ( <i>EcoR</i> I-link)	
<i>bae16B</i> (0.202 kbp)	<i>bae16B</i> for	<u>GAATTCCTCGAACAAGCCGC TTACAAC</u> ( <i>Bam</i> HI)	To construct plasmid T-Bae18
	<i>bae16B</i> rev	<u>GGATCCCAATCCAACCTGCATT CCAGGCCG</u> ( <i>EcoR</i> I-link)	
<i>vbace17</i> (1.862 kbp)	<i>vbace17</i> for	GTGAGAGGCAAAAAGGTATGGATC	To verify <i>bace16-gfp</i> fusion
	<i>vbace17</i> rev	CTTGACAGCTCGTCCATGCCG	
<i>vbae18</i> (1.989 kbp)	<i>vbae18</i> for	GTGGGTTTAGGTAAGAAATTGTCT	To verify <i>bae16-dsRed</i> fusion
	<i>vbae18</i> rev	CATGGTCTTCTCTGCATTAC	
<i>Egfp</i> (0.716 kbp)	<i>egfp</i> for	ATGGTGAGCAAGGGCCGAG	To construct plasmid T-EGFP
	<i>egfp</i> rev	CTTGACAGCTCGTCCATGCCG	

The underlined sequences represent the sites of restriction endonuclease.